FEBS Open Bio 5 (2015) 209–218

FEBS openbio

journal homepage: www.elsevier.com/locate/febsopenbio

Biochemical and spectroscopic properties of *Brucella microti* glutamate decarboxylase, a key component of the glutamate-dependent acid resistance system

Gaia Grassini [a], Eugenia Pennacchietti [a], Francesca Cappadocio [a], Alessandra Occhialini [b,c], Daniela De Biase [a,*]

[a] Istituto Pasteur-Fondazione Cenci Bolognetti, Department of Medico-Surgical Sciences and Biotechnologies, Sapienza University of Rome, 04100 Latina, Italy
[b] Université de Montpellier, Centre d'études d'agents Pathogènes et Biotechnologie pour la Santé (CPBS), F-34293 Montpellier, France
[c] CNRS, FRE 3689, CPBS, F-34293 Montpellier, France

ARTICLE INFO

Article history:
Received 21 January 2015
Revised 11 March 2015
Accepted 12 March 2015

Keywords:
Brucella microti
Glutamate decarboxylase
Cooperativity
pH-dependent activity
Chloride activation
Substituted aldamine

ABSTRACT

In orally acquired bacteria, the ability to counteract extreme acid stress (pH ⩽ 2.5) ensures survival during transit through the animal host stomach. In several neutralophilic bacteria, the glutamate-dependent acid resistance system (GDAR) is the most efficient molecular system in conferring protection from acid stress. In *Escherichia coli* its structural components are either of the two glutamate decarboxylase isoforms (GadA, GadB) and the antiporter, GadC, which imports glutamate and exports γ-aminobutyrate, the decarboxylation product. The system works by consuming protons intracellularly, as part of the decarboxylation reaction, and exporting positive charges via the antiporter.

Herein, biochemical and spectroscopic properties of GadB from *Brucella microti* (*Bm*GadB), a *Brucella* species which possesses GDAR, are described. *B. microti* belongs to a group of lately described and atypical brucellae that possess functional *gadB* and *gadC* genes, unlike the most well-known "classical" *Brucella* species, which include important human pathogens. *Bm*GadB is hexameric at acidic pH. The pH-dependent spectroscopic properties and activity profile, combined with *in silico* sequence comparison with *E. coli* GadB (*Ec*GadB), suggest that *Bm*GadB has the necessary structural requirements for the binding of activating chloride ions at acidic pH and for the closure of its active site at neutral pH. On the contrary, cellular localization analysis, corroborated by sequence inspection, suggests that *Bm*GadB does not undergo membrane recruitment at acidic pH, which was observed in *Ec*GadB. The comparison of GadB from evolutionary distant microorganisms suggests that for this enzyme to be functional in GDAR some structural features must be preserved.

1. Introduction

In several food-borne pathogens and orally acquired bacteria, such as *Escherichia coli*, *Shigella flexneri*, *Listeria monocytogenes* and *Lactoccoccus lactis*, the glutamate-dependent acid resistance system (GDAR) is the most efficient system in counteracting the extreme acid stress encountered by these microorganisms during their transit through the mammalian host stomach [1,2]. GDAR relies on the activities of an enzyme, glutamate decarboxylase (Gad; EC 4.1.1.15), and an antiporter (GadC) (Fig. 1). In *E. coli*, GDAR was extensively studied [1]. Following a drop of the extracellular pH to 2.5 or lower, (i) the cytoplasm becomes acidic (pH ⩽ 5.0) because the cell membrane becomes leaky to protons (H^+); (ii) the intracellular acidification activates Gad, which at each catalytic cycle consumes an intracellular H^+ while converting L-glutamate (L-Glu) into γ-aminobutyrate (GABA); (iii) the proton-consuming activity of Gad is coupled to the electrogenic antiport carried out at this same pH values by GadC, which provides to the L-Glu^0/$GABA^{+1}$ antiport [3,4]. Thus, by consuming H^+ and exporting positive charges, the decarboxylase and the antiporter make up an efficient molecular system which protects the bacteria

Abbreviations: Abs, absorbance; GABA, γ-aminobutyrate; GadB, glutamate decarboxylase (B isoform); *Bm*GadB, *Brucella microti* GadB; *Ec*GadB, *Escherichia coli* GadB; GDAR, glutamate-dependent acid resistance; PLP, pyridoxal 5′-phosphate

* Corresponding author at: Department of Medico-Surgical Sciences and Biotechnologies, Sapienza University of Rome, Corso della Repubblica 79, 04100 Latina, Italy. Tel.: +39 0773 1757212.

E-mail address: daniela.debiase@uniroma1.it (D. De Biase).

http://dx.doi.org/10.1016/j.fob.2015.03.006
2211-5463/

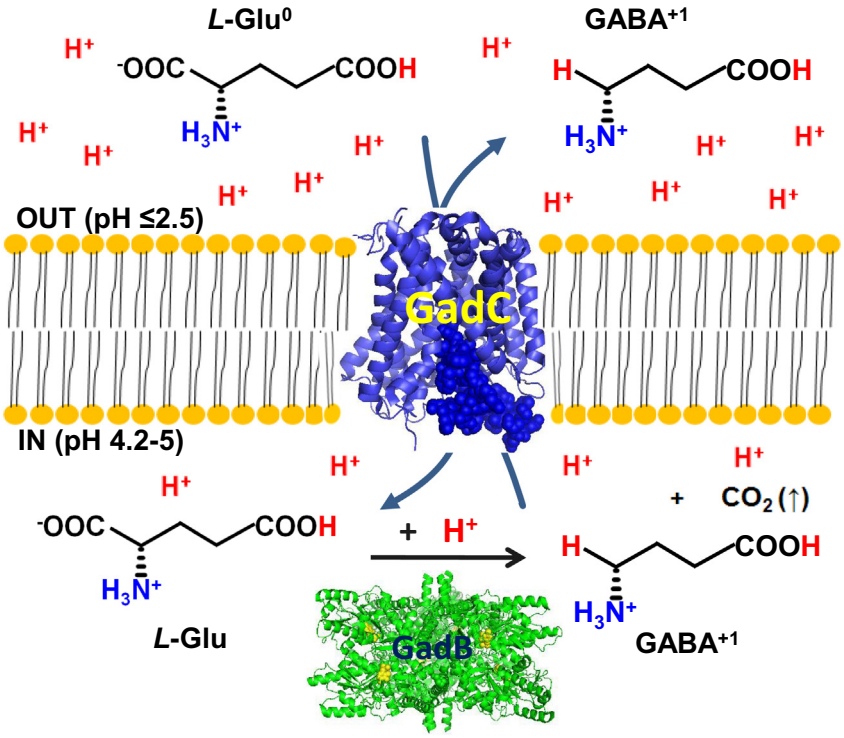

Fig. 1. Schematic representation of the role played by the major structural components of the *E. coli* GDAR system, the most extensively investigated AR system [1]. L-glutamate (L-Glu, net charge 0) is taken up by the electrogenic L-Glu^0/GABA^{+1} antiporter GadC, an inner membrane protein. Decarboxylation of L-Glu via GadA/B consumes an intracellular H^+ at each catalytic cycle, while GadC contributes to the generation of proton motive force by GABA (net charge +1) export. The structures of GadB at acidic pH (PDB: 1PMM) and GadC at pH 8.0 (PDB: 4DJK), the only one currently available, are shown as ribbon drawing generated with PyMol. The C-plug that in GadC is locking the substrate entry channel is shown in filled space.

from a life-threatening acidification of the cytoplasm. The structural bases underlying GadB and GadC activities in *E. coli* have been unveiled and share striking similarities [5,6]. Both proteins undergo auto-inhibition at pH >5.5: GadB uses a 15 amino acid-long C-terminal tail to plug the access to the active site [5], whereas GadC engages the last 41 amino acids residues in its sequence, localized on the cytoplasmic side of the inner membrane, to lock the substrate entry channel [6] (Fig. 1). Notably, in both proteins these structural elements contain histidine residues playing a crucial role as gate-keepers.

While *E. coli* possesses one copy of the GadC coding gene (*gadC*) and two genes (*gadA* and *gadB*) coding for the glutamate decarboxylase isoforms, GadA and GadB, many bacteria possess only one decarboxylase-coding gene (*gadB*) and one antiporter-coding gene (*gadC*), nonetheless they still display GDAR [1]. Amongst them, there is *Brucella microti* CCM4915, an environment-borne pathogenic *Brucella* species isolated from common vole [7], red fox [8] and soil [9], as well as several recently described, atypical *Brucella* species (*Brucella inopinata* BO1 and *B. inopinata*-like BO2 isolated from humans, *Brucella* spp. from African frogs) [10–12] and brucellae isolated from marine mammals (*Brucella ceti* and *Brucella pinnipedialis*).

The *gadB* and *gadC* genes of *B. microti* were recently shown to participate in GDAR [13]: they play an essential role in GDAR *in vitro* and contribute to the survival of *B. microti* in a murine model of infection following oral inoculation. More recently, also the lately described brucellae and those from marine mammals were shown to possess GDAR, unlike the most well-known "classical" terrestrial *Brucella* species pathogenic for livestock, domesticated animals and man (i.e. *Brucella melitensis*, *Brucella abortus*, *Brucella suis*, *Brucella canis* and *Brucella ovis*) [14]. In the "classical" terrestrial species *gadB* and/or *gadC* genes are in fact inactivated by stop codons and/or frameshift mutations [15] and therefore the GDAR system was found to be not functional [14]. The reason for these genotypic differences is still unclear, though it might be related to a specific adaptation of each *Brucella* strain/species to a different environment and to stresses encountered during its lifecycle [14]. This is clearly an interesting aspect if one considers that the World Health Organization has estimated brucellosis as the most widespread bacterial zoonosis [16].

Prompted by (i) the finding that in *B. microti* and many other *Brucella* species GadB participates in GDAR [13,14] and (ii) the new knowledge on the mechanisms controlling the intracellular activity and cellular localization of *Ec*GadB [5,17,18], a detailed biochemical characterization of *B. microti* GadB (*Bm*GadB) was undertaken. *Bm*GadB shares with *E. coli* GadB (*Ec*GadB) 73% sequence identity, including a set of strictly conserved residues which are known to occupy critical positions, i.e. in the active site or at sites where pH-dependent conformational changes occur in *Ec*GadB [1]. In the last decade it was shown that these conformational changes in *Ec*GadB can be clearly monitored spectroscopically and by cellular localization analysis of the protein [5,17,18], thereby avoiding the need to set up more laborious crystallographic investigations. Therefore in this work the kinetic and spectroscopic properties of recombinant *Bm*GadB were compared with those of the thoroughly characterized *Ec*GadB. Overall, our study demonstrates that GadBs from evolutionary distant microorganisms, such as *E. coli* (a Gammaproteobacterium) and *B. microti* (an Alphaprotebacterium), share many biochemical properties and structural features which are instrumental for the full development of GDAR.

2. Materials and methods

2.1. Materials

FastStart High Fidelity PCR system, restriction enzymes, calf intestine alkaline phosphatase, DNA ligation system and ampicillin were from Roche Applied Sciences. StrataClone™ PCR Cloning Kit was from Stratagene. *Taq* DNA polymerase for colony PCR was from GeneSpin (Milano, Italy). Nucleospin® plasmid and Nucleospin® gel and PCR clean-up kits were from Macherey–Nagel. Unstained Protein Molecular Weight Marker for SDS–PAGE was from Thermo Scientific. Ingredients for bacterial growth were from Difco. Streptomycin sulfate was from U.S. Biochemical Corp. (Cleveland, OH, USA). DEAE Sepharose FF was from GE Healthcare Life Sciences. PLP and analytical grade sodium acetate were from VWR International. Sodium chloride was from Riedel-de-Haen. Vitamin B6, potassium dihydrogen phosphate, dipotassium hydrogen phosphate, L-glutamic acid, sodium glutamate and kanamycin were from Fluka. All other chemicals were from Sigma–Aldrich. Oligonucleotide synthesis was by MWG Biotech.

2.2. N-terminal sequence determination

The medium-copy-number plasmid pBBR1MCS-*gadBC* (*B. microti*), consisting of the cloning vector pBBR1MCS carrying a 3.52 kb genome fragment encompassing the whole *B. microti gadBC* operon inclusive of its indigenous promoter [13], was used to transform the *E. coli* strain CC118, which displays extremely low levels of Gad [14], as based on the qualitative GAD test [19] and the quantitative Gad activity assay [20]. Preliminary analysis on the expression and functionality of *Bm*GadB was performed. Briefly, a 50-ml culture was grown overnight (i.e. 18 h) in LB broth at 37 °C. Bacterial cells were collected by centrifugation at 3500 rpm, resuspended in 1 ml of an aqueous solution containing 1 mM PLP/1 mM DTT and disrupted by sonication. The clarified supernatant was subjected to western blotting and Gad activity assay [20,21]. As control, the *E. coli* strain CC118 carrying the empty plasmid pBBR1MCS was analyzed in parallel. Due to the significant degree of protein identity (73%), *Bm*GadB is recognized by the anti-*Ec*GadB antibodies [21]. Using the same protocol described for *Ec*GadB [20], *Bm*GadB was purified to approx. 50% purity from *E. coli* CC118/pBBR1MCS-*gadBC* (*B. microti*) strain. An 11 μg aliquot of partially purified *Bm*GadB (corresponding to approx. 5 μg of pure *Bm*GadB) was subjected to SDS–PAGE [22] followed by blotting onto polyvinylidine difluoride (PVDF) membrane. The area of the PVDF membrane corresponding to *Bm*GadB was excised and subjected to N-terminal sequencing (Proteome Factory AG, Berlin, Germany).

2.3. Cloning strategy

The *B. microti gadB* ORF (i.e. starting from the ATG codon identified by N-terminal sequencing) was amplified using the FastStart High Fidelity PCR system with pBBR1MCS-*gadBC* (*B. microti*) as template and the oligonucleotide pair 5′-GG*CATATG*ACTGGTTCA AACTATCCG-3′ and 5′-GG*GGATCC*TTATGTGTGGTGAAAGCCG-3′ designed to anneal over the start and the stop codons, respectively. The italicized sequences indicate the *Nde*I and *Bam*HI restriction sites used for directional cloning of the PCR product into the corresponding sites of the pET3a expression vector (Novagen). The PCR product was initially cloned into the pSC-A vector (StrataClone PCR Cloning Kit). *E. coli* StrataClone SoloPack transformants were selected by blue/white screening. Plasmids from white colonies were purified and fully sequenced on both strands to check for any unwanted mutation. Plasmid pSC-A_*Bm-gadB* was doubly digested with *Nde*I and *Bam*HI and the resulting 1395-bp DNA fragment, corresponding to the whole *B. microti gadB* ORF, was subcloned into pET3a, previously digested with the same restriction enzymes. The newly generated plasmid pET3a_*Bm-gadB* was used to transform *E. coli* strain DH5α. Transformants were screened for the presence of the insert, initially by colony PCR and then by digestion with *Nde*I and *Bam*HI. For protein expression and purification, the plasmid construct pET3a_*Bm-gadB* was transferred into the *E. coli* strain BL21(DE3), a Gad-negative strain as based on qualitative GAD test [19] and the quantitative Gad activity assay [20].

2.4. Protein purification, SDS–PAGE and cell fractionation

The conditions used for over-expression and purification of *Bm*GadB were essentially as described for *Ec*GadB [20], except that bacteria were grown in LB broth containing 0.5% glucose, induced with 1 mM IPTG and that the DEAE ion-exchange chromatography step was carried out on a smaller-sized column (2.1 cm × 20 cm). Protein purity was assessed by 12% SDS–PAGE [22]. Enzyme concentration and activity were assayed as previously described [20]. The PLP content was determined by releasing it from GadB with 0.1 N NaOH and measuring the absorbance at 388 nm (ε_{388} = 6550 L mol^{-1} cm^{-1}) [23].

The effect of pH on the cellular localization of *Bm*GadB was assessed by SDS–PAGE and enzyme activity in cell extracts from the *E. coli* strain BL21 (DE3)/pET3a_*Bm-gadB* following cell fractionation, as previously described for *Ec*GadB [18]. Briefly, bacteria were grown in 1 L of LB medium, induced with IPTG and harvested by centrifugation at 6000 rpm for 30 min at 4 °C. The bacterial cell pellet was resuspended in 20 ml of 50 mM Tris/HCl pH 7.0, containing 1 mM DTT and protease inhibitors, and split into two 10-ml aliquots. The two samples were brought to pH 7.2 and 5.1 for *Bm*GadB and to pH 7.2 or 5.5 for *Ec*GadB by addition of few microliters of 6 N NaOH or HCl, respectively. After sonication to achieve cell lysis, the pHs of the samples were checked again and adjusted to the correct pH, where necessary. Cell debris was removed by centrifugation at 5000 rpm for 20 min at 20 °C. Hence, the obtained cell supernatants were ultracentrifuged at 50,000 rpm for 1 h at 20 °C to achieve an optimal separation between the cytoplasmic (supernatant) and the membrane (pellet) fractions, which can be separated because the membranes' pellet is firmly bound to the centrifugation tube and from it the supernatant can be completely removed. Each membrane pellet, devoid of any residual liquid phase, was then resuspended in 2 ml of 100 mM Tris/HCl pH 8.0, containing 150 mM NaCl, 5 mM EDTA and 0.5% lauroyl sarcosine. The presence of the detergent is essential to achieve solubilization of the lipids and proteins entrapped in this fraction. Total protein content in each sample was estimated by Micro BCA™ protein assay (Thermo Scientific-Pierce).

2.5. Determination of molecular mass of BmGadB

The molecular mass of recombinant *Bm*GadB was determined by gel filtration at 4 °C using a Superdex 200 10/300 GL column (GE Healthcare, Life Sciences) on an Äkta Prime FPLC system. The mobile phase (50 mM sodium acetate buffer, pH 4.6, containing 150 mM sodium chloride) for column equilibration and protein elution was carried out at a flow rate of 0.5 ml/min. The Gel Filtration HMW Calibration Kit (GE Healthcare, Life Sciences), with the exclusion of thyroglobulin (outside the separation range of the column), was used for column calibration and molecular weight determination. 1 mg of *Bm*GadB was loaded on column.

2.6. GAD activity assay and calculation of kinetic parameters

The specific activity (U/mg) of *Bm*GadB is referred to as μmol GABA min^{-1} mg^{-1} [20]. The k_{cat} and K_m values were determined at 25 °C in 50 mM sodium acetate buffer, pH 4.6, containing 40 μM PLP. The Gabase assay was used to measure GABA production at time intervals [20]. Briefly, *Ec*GadB (0.5 μg) or *Bm*GadB (3 μg) were incubated with 0.3–30 mM L-glutamate. The reaction rate was determined by measuring the production of GABA in the first 3 min of reaction. The data collected were fitted to the standard Michaelis–Menten equation as in GraphPad Prism 4.0.

2.7. Spectroscopic measurements and data analysis

Enzyme absorption spectra were recorded at room temperature on a Hewlett–Packard Agilent model 8453 diode array spectrophotometer. The buffer systems used for titrations were the followings: 50 mM sodium acetate buffer in the pH range 3.5–5.8 and potassium phosphate buffer in the pH range 6.0–7.0.

Fluorescence excitation and emission spectra were recorded with a FluoroMax-3 spectrofluorometer (Horiba Jobin–Yvon) equipped with a thermostatically controlled cell compartment at 20 °C using 5 nm bandwidth on both slits (2 nm, when excited at 295 nm) and at a scan speed of 100 nm/min. The spectra were corrected by subtracting the corresponding buffer spectrum.

Curve fitting and statistical analyses were carried out with GraphPad Prism 4.0 (GraphPad Software, San Diego, CA). The pH-dependent absorbance (Abs) changes at 420 nm and 340 nm were analyzed using Hill equation as provided in GraphPad Prism, in which *pK* is the pH at the midpoint of the spectroscopic transition and *n* is the number of protons (i.e. Hill coefficient) required for the transition.

2.8. Bioinformatic analysis

Sequence alignments were performed using Clustal Omega (http://www.ebi.ac.uk/Tools/msa/clustalo/). Secondary structure predictions and protein parameters were obtained using resources accessible from Expasy (http://expasy.org/proteomics).

3. Results

3.1. Over-expression and purification of BmGadB

The amino acid sequence of *Bm*GadB from the NCBI and Patric [24] databases differs in the N-terminal region (Fig. 2). In the NCBI database *Bm*GadB (NCBI: YP_003105130.1) is reported to be 6 amino acids longer at the N-terminal end than *Ec*GadB, whereas in the Patric database the amino acid sequence is two residues shorter than that of *Ec*GadB.

In order to experimentally validate the N-terminal sequence, *Bm*GadB were partially purified (i.e. 50% purity) following its overproduction in the *E. coli* strain CC118 carrying plasmid pBBR1MCS-*gadBC* (*B. microti*). This construct consists of the cloning vector pBBR1MCS carrying the *B. microti gadBC* operon [13]. The expression and functionality of *Bm*GadB were assessed as described in Materials and Methods. Following electroblotting onto PVDF membrane, the protein band corresponding to *Bm*GadB (5 μg; 94 pmol) was subjected to Edman degradation and the N-terminal sequence Met-Thr-Gly-Ser-Asn confirmed that the correct N-terminal sequence was that provided in Patric [24]. Thus mature *Bm*GadB consists of 464 amino acids (Fig. 2) and its molecular weight is predicted to be 52,184 Da.

Following the identification of the correct N-terminal sequence, plasmid pET3a_*Bm-gadB* was constructed and used to transform *E. coli* BL21(DE3), a commonly employed pET system expression host. The choice of this host strain for the expression of *Bm*GadB was also based on the finding that it is GAD-negative using a qualitative GAD test [13,19]. At present the reason for possessing a GAD-negative phenotype is unknown. In fact, the publicly available genome sequence of *E. coli* BL21(DE3) indicate that endogenous *gadA* and *gadB* genes are both present and intact. Thus Gad-negative phenotype might arise either from the single nucleotide polymorphisms detected in the promoter region of *gadA* (at position −50 relative to the transcription start site) and *gadB* (at position −190 relative to the transcription start site) genes or from reduced activity/expression of the transcriptional regulators necessary to trigger the expression of the GDAR system [25].

Purification of *Bm*GadB was carried out essentially following the protocol used for *Ec*GadB [20] and yielded approximately 10 mg of soluble protein from a 2-Liter bacterial culture, even though most of the overexpressed protein was in the form of insoluble material. *Bm*GadB was judged by SDS–PAGE to be 95% pure and to contain the full complement (100%) of bound PLP.

Under the standard assay conditions used for *Ec*GadB (50 mM sodium glutamate in 0.2 M pyridine/HCl buffer, pH 4.6, containing 0.1 mM PLP, at 37 °C), the specific activity of *Bm*GadB was 190 Units/mg, a value close to that of the *E. coli* counterpart. The k_{cat} and K_m values calculated for *Bm*GadB are provided in Table 1. Compared to *Ec*GadB, K_m of *Bm*GadB is 2.4 times higher, whereas k_{cat} is similar, thus resulting in an enzyme with a specificity constant k_{cat}/K_m halved respect to that of *Ec*GadB.

Purified recombinant *Bm*GadB has an apparent molecular mass of 52 kDa as based by SDS–PAGE (data not shown) and elutes as a 307.4-kDa species by gel filtration chromatography carried out at pH 4.6 on a Superdex 200 10/300 column (Fig. 3). These results indicate that at acidic pH, that is when the enzyme is maximally active (see next section), *Bm*GadB is a hexamer, alike *Ec*GadB.

3.2. pH-dependent absorbance and activity changes

*Bm*GadB undergoes distinct pH-dependent spectroscopic changes in the region of the UV–visible spectrum where the PLP cofactor absorbs (Fig. 4A), and these resemble those of *Ec*GadB [17]. The absorption spectra recorded in the pH range 3.5–6.5 provide evidence that the cofactor absorbance maximum abruptly shifts from 420 nm (corresponding to the ketoenamine, active form) to 340 nm (corresponding to the substituted aldamine, inactive form) in the narrow pH range 4.4–5.2. Thus the only noticeable difference respect to *Ec*GadB [5,17,26] consists in the slightly more acidic pH range at which the 420 ↔ 340 nm shift in absorbance occurs (Table 2), though the characteristic isosbestic point of the spectroscopic transition at 361 nm remains unaffected [17].

The titration curve generated by fitting the absorbance values at 420-nm versus pH is shown in Fig. 4B and exhibits a sigmoidal dependence which can be fitted by the Hill equation. The best-fit values returned for number of protons (*n*) and midpoint pH (*pK*) of the spectroscopic transition are given in Table 2 where corresponding numbers for *Ec*GadB are also provided for comparison. As mentioned above, the pH-dependent spectroscopic transition of *Bm*GadB occurs at more acidic pH than *Ec*GadB and is complete at pH 5.5 (Fig. 4B), where the 420-nm absorbing species becomes barely detectable (Fig. 4A). This latter observation is indicative of an efficient locking of the active site in *Bm*GadB, a finding substantiated by the activity assays (see below).

Chloride ions and other halides were reported to bind at allosteric sites in *Ec*GadB thereby stabilizing the 420-nm, active form [5,26]. When a similar analysis was carried out on *Bm*GadB, it was observed that the cofactor spectroscopic transition is similarly affected by chloride ions (Fig. 4B): the 420-nm species persists up to pH 5.2 and the *pK* of the spectroscopic transition is increased by

```
E. coli      ------MDKKQVTDLRSELLDSRFGAKSISTIAESKRFPLHEMRDDVAFQIINDELYLDG   54
B. microti   MKITLEVIMTGSNYPARDLIASVFGTEALQEIAASRGFPEKEMQANAVYQIIHDELFLDG   52
                   :  .  .    :*: * **:::::. ** *: ** :**: :..:***.***:***

E. coli      NARQNLATFCQTWDDENVHKLMDLSINKNWIDKEEYPQSAAIDLRCVNMVADLWHAPAPK  114
B. microti   NARQNLATFCQTWDDDYVHKLMDLSINKNWIDKEEYPQSAAIDLRCVNMVADLWNAPKFA  112
             ***************: ************************************.**

E. coli      NGQAVGTNTIGSSEACMLGGMAMKWRWRKRMEAAGKPTDKPNLVCGPVQICWHKFARYWD  174
B. microti   -DNATGTNTIGSSEACMLGGMAMKWRWRKKMQEMGKPTDKPNFVCGPVQVCWHKFARYWD  171
               :*.************************:*:  ********:******:**********

E. coli      VELREIPMRPGQLFMDPKRMIEACDENTIGVVPTFGVTYTGNYEFPQPLHDALDKFQADT  234
B. microti   VEIREIPMEPGRLFMGPEQMLEAVDENTIGVVPTFGVTYTGNYEFPEPLQDALDKLQKTK  231
             **:*****.**:*** *::*:** **********************:**:*****:*  .

E. coli      GIDIDMHIDAASGGFLAPFVAPDIVWDFRLPRVKSISASGHKFGLAPLGCGWVIWRDEEA  294
B. microti   GLDIDIHVDAASGGFLAPFCAPDIPWDFRLPRVKSISASGHKYGLAPLGCGWVVWRDKEA  291
             *:***:*:*********** **** ****************:**********:***:**

E. coli      LPQELVFNVDYLGGQIGTFAINFSRPAGQVIAQYYEFLRLGREGYTKVQNASYQVAAYLA  354
B. microti   LPEELIFNVDYLGGQVGTFAINFSRPAGQVISQYYEFMRLGREGYTKVQQAAYRVAQYIA  351
             **:**:*********:***************:*****:**********:*:*:** *:*

E. coli      DEIAKLGPYEFICTGRPDEGIPAVCFKLKDGEDPGYTLYDLSERLRLRGWQVPAFTLGGE  414
B. microti   REIEPLGPYEFICAGEEKGGIPAVCFRIREGEDPGYSLYDLSERLRLTGWQVPAFALSGK  411
              **  ********:*. . *******::::******:********** *******:*.*:

E. coli      ATDIVVMRIMCRRGFEMDFAELLLEDYKASLKYLSDHPKLQGIAQ-QNSFKHT         466
B. microti   ASDITVMRVMCRRGFEMDLAALFIRDFKAGIEFFKSHPSPKITPSMGTGFHHT         464
             *:**.***:*********:* *::.*:**.::::..**. :   .  ..*:**
```

Fig. 2. Clustal Omega (version 1.2.1) alignment of *Ec*GadB and *Bm*GadB. The residues in bold blue in *Bm*GadB correspond to the N-terminal sequence experimentally determined by Edman degradation and on which numbering is based. The first 8 amino acids (in italics) in *Bm*GadB are those reported in the NCBI database (Reference Sequence: YP_003105130.1), but absent in the protein sequence. The amino acid residues corresponding to the regions that in *Ec*GadB undergo the most noticeable conformational changes are red. The residues participating in halide binding in *Ec*GadB [5] are in green background.

Table 1
Kinetic parameters of *Bm*GadB compared to those of *Ec*GadB.

	k_{cat} (s^{-1})	K_m (mM)	k_{cat}/K_m (s^{-1} mM^{-1})
*Bm*GadB	17.88 ± 0.31	2.68 ± 0.17	6.66 ± 0.53
*Ec*GadB	15.28 ± 0.58	1.10 ± 0.18	13.92 ± 2.83

The values reported were calculated using the integrated Michaelis–Menten equation as provided in GraphPad Prism 4.0.

0.45 pH units (Table 2). These results are consistent with the observation that the residues that in *Ec*GadB were shown to be involved in halides binding [5] are conserved in *Bm*GadB (Fig. 2).

To assess whether the pH dependency of the activity of *Bm*GadB matches that of the UV–visible spectroscopic changes, Gad activity assays were performed in the absence/presence of sodium chloride in the pH range 3.8–6.5. As shown in Fig. 5, *Bm*GadB displays its maximal activity at low pH, but only up to pH 4.5. At pH ∼5 the enzyme exhibits 50% of the activity measured at pH 3.8–4.5 and activity becomes undetectable at a pH higher than 5.6. Notably, in the pH range 3.8–5.3 *Bm*GadB is 1.5–3 times more active when chloride ions are present (Fig. 5). This is similar to what is observed with *Ec*GadB (Fig. 5, inset), except that in *Ec*GadB 50% of the activity is detected at pH 5.24 and 5.32, whereas that of *Bm*GadB was detected at pH 4.95–5.13 in the absence and presence of chloride ions, respectively. For both proteins the data of activity versus pH fit well to the Hill equation, suggesting that cooperativity occurs, as previously shown [17]. However a shift of 0.45 pH units in the *pK* of the spectroscopic transitions observed in the presence of chloride ions (Fig. 4B and Table 2) has not been observed on the pH at which 50% of activity is detected. In other words chloride ions stabilize the active form of the enzyme and enhance the activity of *Bm*GadB, but their presence does not cause a shift towards neutral pH of the half-maximal activity value. This suggests that the deprotonation state of active site residues is the one mostly responsible for restricting the range of enzyme activity. A similar observation was made for *Ec*GadB [17].

3.3. Fluorescence properties

For *Ec*GadB spectrofluorometric analysis has provided useful insights into the chemical state of the cofactor as a function of pH [17]. When *Bm*GadB is excited at pH 4.0 at 430 nm, the emission spectrum (with a maximum at 500 nm) is typical of the ketoenamine tautomer of internal aldimine, which on the contrary is barely detectable when the enzyme is excited at the same wavelength but at neutral pH (Fig. 6A). These data are similar to those reported for *Ec*GadB [17] and, together with the UV–visible spectra, confirm that the active form of *Bm*GadB has internal aldimine protonated on the imine nitrogen, a pre-requisite for being catalytically competent.

In order to obtain evidence on the chemical state of the inactive enzyme form absorbing at 340 nm (Fig. 4A), the emission spectrum of *Bm*GadB, following excitation at either 295 nm or 345 nm, was recorded both at acidic and near-to-neutrality pH (Fig. 6B and C). It is important to recall here that in *Ec*GadB His465 is responsible for the formation of a substituted aldamine at pH >5.5 [5]. This species emits with a maximum at 350 nm and 400 nm when excited at 295 nm and 345 nm, respectively [17]. Instead, the *Ec*GadB

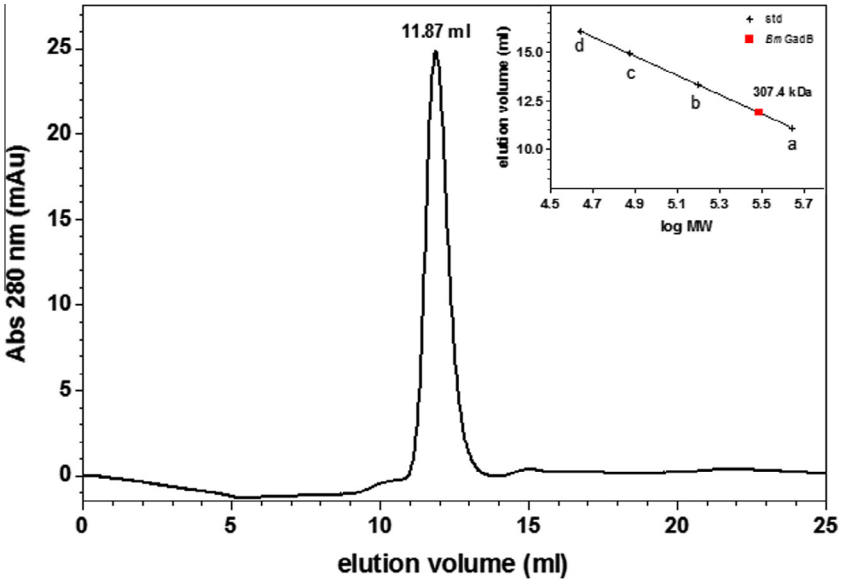

Fig. 3. Determination of molecular mass of *Bm*GadB. Gel filtration chromatography of *Bm*GadB (shown as red square on the calibration curve) on a Superdex 200 10/300 GL (GE Healthcare) column was carried out in 50 mM sodium acetate buffer, pH 4.5, containing 150 mM NaCl, at a flow rate of 0.5 ml/min. HMW Calibration Kit (GE Healthcare) included ferritin (440 kDa; a), aldolase (158 kDa; b), conalbumin (75 kDa; c), ovalbumin (44 kDa; d). 1 mg of *Bm*GadB was loaded on the column immediately after calibration.

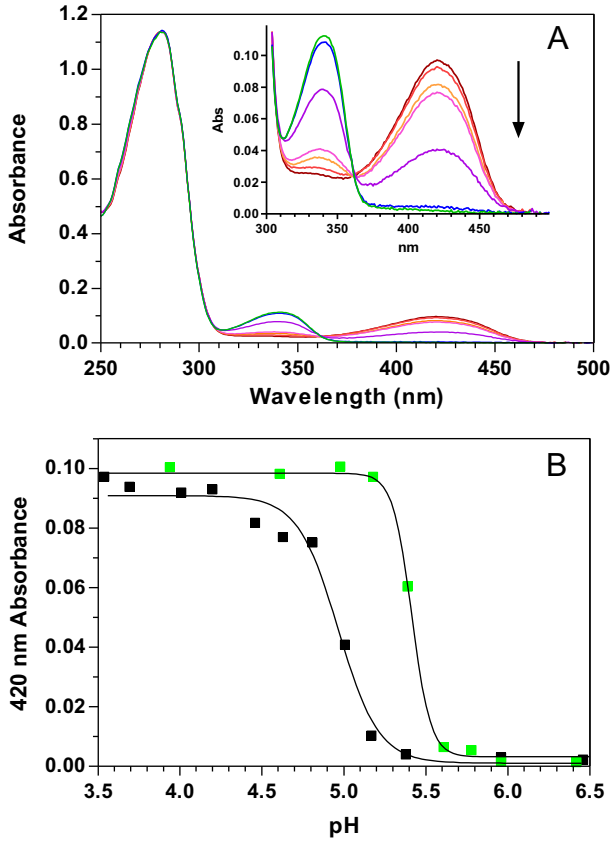

Fig. 4. pH-dependent absorbance changes. (A) Absorption spectra of *Bm*GadB were recorded in 50 mM sodium acetate buffer at pH 3.5 (dark red), 4.2 (red), 4.5 (orange), 4.6 (magenta), 5.0 (violet), 5.4 (blue) and in 50 mM potassium phosphate buffer at pH 6.5 (green). Spectra were normalized taking into account the full PLP content (11.6 μM). The arrow indicates the direction of the change in absorbance at 420 nm upon pH increase. Inset: zoom of the 300–500 nm region. (B) The pH-dependent change in absorbance at 420 nm is represented in the absence (black squares) and presence (green squares) of 50 mM NaCl. The solid lines through the experimental points show the theoretical curves obtained using Hill equation as in GraphPad Prism 4.0.

Table 2
Hill parameters from curve fitting of the 420 nm absorbance readings as a function of pH.

	n	*pK*
*Bm*GadB	3.52 ± 0.67	4.965 ± 0.028
*Bm*GadB + 50 mM NaCl	7.52 ± 1.58	5.414 ± 0.008
*Ec*GadB	9.64 ± 0.99	5.337 ± 0.004
*Ec*GadB + 50 mM NaCl	7.86 ± 0.59	5.720 ± 0.005

The values reported were calculated using the integrated Hill equation.

His465Ala variant exhibits a second emission band at 500–510 nm (Fig. 6C). This is characteristic of the enolimine tautomer of the internal aldimine, that is the species with the hydrogen on the phenolic oxygen more typical in a less polar environment ([17] and references therein).

Fluorescence emission spectra recorded upon excitation either at 295 nm (Fig. 6B) or at 345 nm (Fig. 6C) provide a clear indication that at pH 6.5 in *Bm*GadB a substituted aldamine is formed. In fact the emission band at 500–510 nm is never detected (Fig. 6B and C).

3.4. pH-dependent cellular partition

In *Ec*GadB two triple helical bundles, formed at acidic pH by the N-terminal residues 3–15 of each subunit, were shown to be involved in recruiting the decarboxylase to the cytosolic side of the inner membrane, the cellular compartment where the relieving effect from protons' consumption was suggested to be more beneficial to the acid-stressed cell [5,18]. In addition these structural elements provide proper orientation of side-chains of residues involved in the binding of chloride ions, which act as allosteric activators.

Secondary structure prediction tools indicate that the N-terminal sequence of *Bm*GadB (which contains a Pro residue at position 7) does not support formation of α-helices. Conversely, the same tools predict the N-terminal region of *Ec*GadB to be able to form α-helices and this agrees with the crystal structure data [18]. Despite the apparent inability to form an α-helix in the N-terminal region, *Bm*GadB might still retain the ability to partition

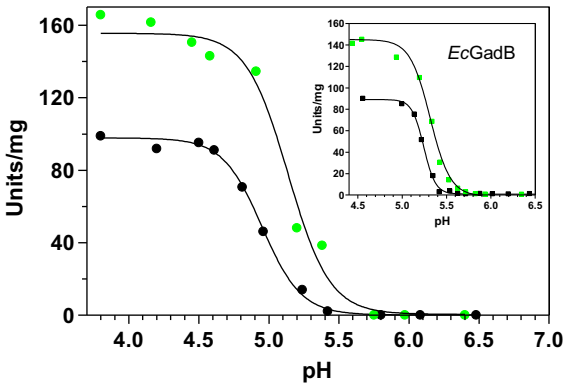

Fig. 5. Effect of pH on the activity of *Bm*GadB. Gad activity (Units mg^{-1}) was measured at 37 °C in 50 mM sodium acetate (pH 3.8–5.8) or phosphate (pH 6.0–6.5) buffer containing 40 μM PLP, 50 mM glutamate and in the absence (black circles) or presence (green circles) of 50 mM NaCl. The protein concentration was 0.5–2 μM. The solid lines through the experimental points represent the theoretical curves obtained using Hill equation to fit the data. The same experiment but with *Ec*GadB is shown in the inset.

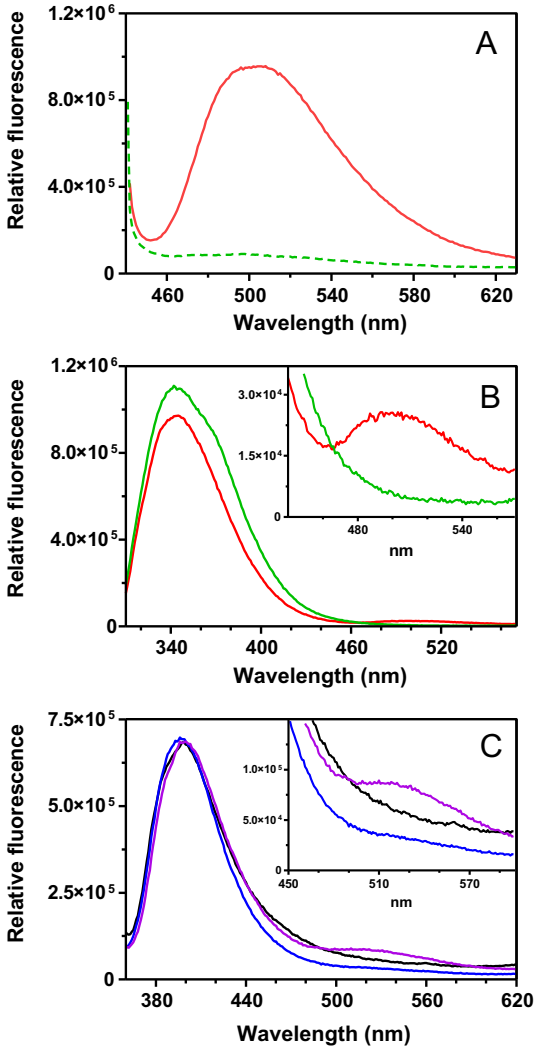

Fig. 6. Fluorescence emission spectra of *Bm*GadB. Emission spectra were recorded at pH 4.0 (red line) and at pH 6.5 (green line) following excitation at 430 nm (A) and 295 nm (B). (C) Emission spectra of *Bm*GadB (black line), *Ec*GadB (blue line) and *E. coli* GadBH465A (violet line) were recorded following excitation at 345 nm at pH 6.5. The protein concentration of *Bm*GadB was 13 μM. The protein concentration of *Ec*GadB and GadBH465A was 3 μM. The buffers used were 50 mM sodium acetate at pH 4.0 and 50 mM potassium phosphate at pH 6.5.

between the cytosol and the membrane following a decrease in cytoplasmic pH. In order to address this point, cell fractionation of the *E. coli* BL21(DE3) overexpressing *Bm*GadB was carried out. Cytoplasmic and membrane fractions at neutral pH and at pH 5.1, in the presence of chloride, were assayed for enzyme activity and analyzed by SDS–PAGE (Fig. 7). The same analysis was carried out on an *E. coli* strain overexpressing *Ec*GadB, as previously reported [18]. The pH 5.1 was chosen for *Bm*GadB because at this pH the enzyme is still in the active form (Fig. 5 and Table 2). As predicted on the basis of the N-terminal amino acid sequence, the cellular localization of *Bm*GadB is not influenced by a pH decrease, unlike that of *Ec*GadB (Fig. 7 and [18]), thus suggesting that in *Bm*GadB the N-terminal region does not undergo the same conformational changes which were reported to occur in *Ec*GadB. Notably, a significant fraction of the protein (approximately 40%) is associated to the membrane already at neutral pH and no further recruitment to the membrane is observed when the pH of the cell extract is lowered to 5.1.

4. Discussion

After the discovery that Gad is a major structural component of GDAR [21,27–32], only Gad from *E. coli* was investigated in detail at the spectroscopic, biochemical and structural level [5,17,18,33]. However it is becoming clear that GDAR is amongst the most potent acid resistance systems in several neutralophilic bacteria [1,2]: the acidic pH optimum of Gad as well as the nature of the substrate and the product are best suited to protect bacteria from the uncontrolled acidification of the cytoplasm occurring upon exposure to harsh acid stress. Thus the molecular mechanisms underlying the control of Gad intracellular activity in different bacterial species is of particular interest, especially from the evolutionary viewpoint.

In order to fill this lack of knowledge, purification and biochemical characterization of recombinant GadB from *B. microti* (*Bm*GadB) was undertaken. The genus *Brucella*, belonging to the class Alphaproteobacteria, consists of Gram-negative, facultative intracellular coccobacilli, highly pathogenic for a variety of mammals, including humans [16]. The twelve species of the genus are classified on the basis of specific phenotypic traits and their natural host preferences and grouped into "classical" and "newly described, atypical" species, depending on the year of discovery and description (more or less than twenty years). Humans brucellosis, also known as Malta fever, is essentially acquired by the oral route, following the ingestion of non-pasteurized milk and dairy products, but also *via* respiratory and conjunctival mucosae. Thus, during their lifecycle these bacteria must cope with quite acidic environments such as those encountered in fermented foods, in the gastrointestinal tract of their hosts or in the intracellular vacuole.

*Bm*GadB was chosen for an in-depth biochemical and spectroscopic characterization because its role in *B. microti* GDAR has been clearly established [13]. Moreover *B. microti* belongs to a group of "newly described" *Brucella* species that possess functional *gadB* and *gadC* genes, thus distinct from the "classical" *Brucella* species (which includes species described at least twenty years ago) in which the same genes are not functional because of the occurrence of stop codons and/or frameshift mutations in their ORFs [15]. In the absence of clinical cases in humans and farm animals, the pathogenicity of these bacteria remains unknown. However with respect to the "classical" *Brucella* species, the newly described brucellae share some characteristics such as the higher metabolic activities, which lead to faster growth, the ability to resist better to extreme acid stress, higher replication rates in murine and human macrophages, and the lethality in a mouse model of

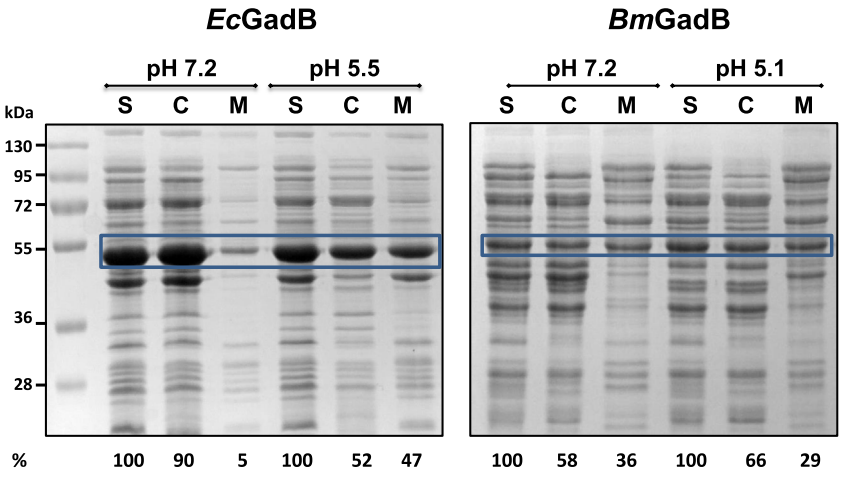

Fig. 7. pH dependent cellular partition in *Ec*GadB (left panel) and *Bm*GadB (right panel). 12% SDS–PAGE of 30 μg-samples of cell supernatants (S), obtained after cell lysis, cytoplasmic (C) and membrane (M) fractions obtained as described in Section 2.4 at neutral (pH 7.2) and mildly acidic pH (pH 5.5 *Ec*GadB or pH 5.1 *Bm*GadB). The region of the gel encompassing the bands corresponding to *Ec*GadB and *Bm*GadB is shown with a blue box. Molecular weight (kDa) standards are shown on the *right* of the left panel. The decarboxylase activity is provided as percentage with respect to the corresponding starting activity in S (100%). The reported activity values represent the mean of 2–3 independent experiments, with a standard deviation not exceeding 10% of the stated value.

infection for at least some of them [13,14,34–36]. Regarding acid stress response, it is thus noticeable that GDAR is present in "new and atypical" brucellae and also in several strains of *B. ceti* and *B. pinnipedialis* isolated from marine mammals [13,14], while absent in the terrestrial "classical" ones. This is apparently contradictory taking into account that in humans the oral route is the major route of infection of the "classical" species and that humans are only accidental hosts. In addition, it was suggested that these bacteria can pass into the bloodstream through the tonsils, already before reaching the gastrointestinal tract where other acid resistance factors, such as the urease enzyme, may also occur [37]. Our hypothesis is that, starting from a GAD-positive *Brucella* ancestor, this phenotypic trait was conserved in the "new and atypical" brucellae to increase their fitness and versatility and that it was lost in the classical highly pathogenic species adapted to specific hosts, except in the brucellae isolated from marine mammals [14].

Based on the above findings, information on the biochemical properties of GadB, an important structural element of GDAR, may provide useful information to better understand the biology and the transmission of "new and atypical" brucellae isolated from the environment and wildlife. It is in fact important to know better these *Brucella* species which now include strains isolated from non-mammals, African frogs [10]. In the present work, the biochemical and spectroscopic properties of *Bm*GadB were compared with those of the thoroughly characterized *Ec*GadB [1] with which it shares 73% sequence identity. The level of purity of *Bm*GadB (>95% as based by SDS–PAGE and spectroscopic measurements) was essential to carry out a comparison with *Ec*GadB. Similarities of *Bm*GadB with the *E. coli* homolog include the hexameric assembly at acidic pH and the ability to undergo pH-dependent spectroscopic and activity changes, both affected by chloride ions. UV–visible and fluorescence emission spectra provide also a clear indication that at neutral pH the cofactor PLP in the active site of *Bm*GadB is present as substituted aldamine, thus suggesting that the reversible inactivation mechanism which was shown to occur in *Ec*GadB [5,17] is conserved in *Bm*GadB too.

The sequence alignment in Fig. 2 reveals that *Bm*GadB mostly diverges from *Ec*GadB in the 15–20-amino acids located in the N-terminal and C-terminal portions, with the notable exception of residues Ser14, Phe16, Gly17, Pro449, Phe461, His463 and Thr464. The corresponding residues in the sequence of *Ec*GadB are Ser16, Phe18 and Gly19, involved in chloride ions binding, and Pro452, Phe463, His465 and Thr466 belonging to the C-terminal tail involved in active site closure at neutral pH and providing the residue His465, in the last but one position, which is responsible for aldamine formation [5,17]. Notably, in *Bm*GadB two are the candidate histidines for aldamine formation, i.e. His462 and His463, in the last but two and penultimate position in sequence, respectively (Fig. 2). At present none of the candidates can be unequivocally assigned as the one responsible for aldamine formation. However, as shown in Fig. 2 and based on the multiple sequence alignment of bacterial Gads (Fig. 1S in [1]), His463 is proposed to be the most likely candidate. Thus His463 should occupy a position structurally equivalent to His465 in *Ec*GadB, responsible for locking the active site at pH >5.3 (pH >5.7 in the presence of chloride ions) [5,17].

As far as the N-terminal region of *Bm*GadB is concerned, it does not display a propensity to form triple helical bundles at acidic pH. The formation of these structural elements requires a hydrophobic core and polar/charged residues on the outside [18]. Furthermore the residues corresponding to Asp2, Asp8 and Asp15 of *Ec*GadB, the protonation of which is likely required to drive the formation of the triple helices at acidic pH, are lacking. In addition a proline residue in the 7th position is further contrasting the acquisition of a helical arrangement (Fig. 2). The analysis of the partition of the protein between the membrane and cytosolic fractions did not show any effect of acid pH and this is in line with the inability to form the triple helical bundles. Nonetheless, *Bm*GadB retains the ability to bind and be affected by chloride ions (Table 2, Figs. 4 and 5), which act as positive allosteric effectors. This is corroborated by the inspection of the protein sequence in which all the residues that in the crystal structure of *Ec*GadB were shown to be involved in halides binding are conserved in *Bm*GadB. Thus the ability of binding chloride ions (typically abundant in the stomach) is still possible and is unlinked to the formation of triple helical bundles in the N-terminal region. The amino acid conservation and the remarkable similarities of the effect of these anions on *Ec*GadB and *Bm*GadB (Figs. 4 and 5) is strongly in favor of this hypothesis, even in the absence of crystal structure [5,18].

The fact that *Bm*GadB is already localized in the membrane fraction at neutral pH still fits with the model of GadB functioning in acid stress response. In fact even though *Bm*GadB is not significantly affected by acidic pH, 30–40% of the total enzyme in the membrane fraction, regardless of the pH, should be enough to accomplish the acid protective function. In addition, chloride ions were found to be very strong allosteric activators of the enzyme.

Therefore the activity of *Bm*GadB in the membrane can also be modulated by other factors, besides membrane recruitment.

As already pointed out in recent reports on the evolutionary history of the *Brucella* genus, which likely occurred as explosive radiation [38,39], both *B. inopinata* BO1 and *B. inopinata*-like BO2 isolated from humans, are amongst the oldest brucellae. Both possess functional GDAR and their GadB displays full activity [14]. Sequence alignment of GadB from all the *Brucella* species with a functional GDAR and available genome sequence, i.e. *B. inopinata* BO1, *B. inopinata*-like BO2, *B. ceti*, *B. pinnipedialis* and *B. microti*, indicates that *B. inopinata* BO1 is the most distant (data not shown). However, none of the amino acid mutations reported in *B. inopinata* BO1 (5/464; 1.08%) affects the amino acid residues constituting the Gad signature or the residues involved in halides binding. It is therefore likely that GadB from any of the *Brucella* species with a functional GDAR shares same spectroscopic, biochemical and functional properties with *Bm*GadB.

To the best of our knowledge, *Bm*GadB and *Ec*GadB are the only Gad from evolutionary distant bacteria that have been characterized in detail, especially with respect to the pH-dependent spectroscopic and functional properties important for GDAR. More than forty years ago interesting biochemical reports on Gad from vegetative cells of *Clostridium perfringens*, an anaerobic Gram-positive bacterium, belonging to the phylum Firmicutes, were published [40–44]. However none of the features described for the *E. coli* and *B. microti* homologs were reported. *C. perfringens* in addition to being normal inhabitant of the human gut is also a causative agent of food poisoning in humans. The ability of *C. perfringens* vegetative cells and spores to survive from gastric acidity was investigated in recent years [45]: spores, which are responsible for the formation of the endotoxin involved in the poisoning symptoms, are much less resistant to gastric acidity, unlike vegetative cells which are still capable of surviving acid stress to a significant extent. Notably *C. perfringens* possesses both *gadB* (CPE2058) and *gadC* (CPE2060) genes, separated by the gene CPE2059 likely involved in the protection from acid stress [1]. In light of a possible involvement of *C. perfringens* Gad in GDAR and in the successful colonization of the gut, expression and biochemical studies on this Gad should be reconsidered.

5. Conclusions

The biochemical and spectroscopic properties of *Bm*GadB provide evidence that GadB, a key component of glutamate-dependent acid resistance (GDAR) in many new and atypical *Brucella* species and in those from marine mammals, shares many features with the *E. coli* homolog, *Ec*GadB, which was extensively characterized at the biochemical and structural level. These features are therefore regarded as instrumental for proper functioning of GDAR in these bacteria.

Acknowledgments

The authors thank Dr. Stephan Köhler for critically reading the manuscript. This work was in part supported by Fondazione Roma (to DDB). Mobility of AO and DDB was supported by the 2011–2012 Galilée program of Egide (Hubert Curien program) n 25960UE from the French and Italian Ministry of Foreign and Europeans Affairs. GG and EP were recipients of a bursary from the Istituto Pasteur-Fondazione Cenci Bolognetti.

Authors contribution: GG, performed experiments, analyzed data and wrote first draft of paper; EP, performed experiments and analyzed data; FC, performed experiments; AO, contributed reagents and helped in manuscript writing; DDB, conceived and designed the project, analyzed the data and wrote the paper.

References

[1] De Biase, D. and Pennacchietti, E. (2012) Glutamate decarboxylase-dependent acid resistance in orally acquired bacteria: function, distribution and biomedical implications of the *gadBC* operon. Mol. Microbiol. 86, 770–786.
[2] Lund, P., Tramonti, A. and De Biase, D. (2014) Coping with low pH: molecular strategies in neutralophilic bacteria. FEMS Microbiol. Rev. 38, 1091–1125.
[3] Tsai, M.F., McCarthy, P. and Miller, C. (2013) Substrate selectivity in glutamate-dependent acid resistance in enteric bacteria. Proc. Natl. Acad. Sci. U S A 110, 5898–5902.
[4] Ma, D., Lu, P. and Shi, Y. (2013) Substrate selectivity of the acid-activated glutamate/gamma-aminobutyric acid (GABA) antiporter GadC from *Escherichia coli*. J. Biol. Chem. 288, 15148–15153.
[5] Gut, H., Pennacchietti, E., John, R.A., Bossa, F., Capitani, G., De Biase, D. and Grutter, M.G. (2006) *Escherichia coli* acid resistance: pH-sensing, activation by chloride and autoinhibition in GadB. EMBO J. 25, 2643–2651.
[6] Ma, D., Lu, P., Yan, C., Fan, C., Yin, P., Wang, J. and Shi, Y. (2012) Structure and mechanism of a glutamate-GABA antiporter. Nature 483, 632–636.
[7] Scholz, H.C., Hubalek, Z., Sedlacek, I., Vergnaud, G., Tomaso, H., Al Dahouk, S., Melzer, F., Kampfer, P., Neubauer, H., Cloeckaert, A., Maquart, M., Zygmunt, M.S., Whatmore, A.M., Falsen, E., Bahn, P., Gollner, C., Pfeffer, M., Huber, B., Busse, H.J. and Nockler, K. (2008) *Brucella microti* sp. nov., isolated from the common vole *Microtus arvalis*. Int. J. Syst. Evol. Microbiol. 58, 375–382.
[8] Scholz, H.C., Hofer, E., Vergnaud, G., Le Fleche, P., Whatmore, A.M., Al Dahouk, S., Pfeffer, M., Kruger, M., Cloeckaert, A. and Tomaso, H. (2009) Isolation of *Brucella microti* from mandibular lymph nodes of red foxes *Vulpes vulpes*, in lower Austria. Vector Borne Zoonotic Dis. 9, 153–156.
[9] Scholz, H.C., Hubalek, Z., Nesvadbova, J., Tomaso, H., Vergnaud, G., Le Fleche, P., Whatmore, A.M., Al Dahouk, S., Kruger, M., Lodri, C. and Pfeffer, M. (2008) Isolation of *Brucella microti* from soil. Emerg. Infect. Dis. 14, 1316–1317.
[10] Eisenberg, T., Hamann, H.P., Kaim, U., Schlez, K., Seeger, H., Schauerte, N., Melzer, F., Tomaso, H., Scholz, H.C., Koylass, M.S., Whatmore, A.M. and Zschock, M. (2012) Isolation of potentially novel *Brucella* spp. from frogs. Appl. Environ. Microb. 78, 3753–3755.
[11] Tiller, R.V., Gee, J.E., Lonsway, D.R., Gribble, S., Bell, S.C., Jennison, A.V., Bates, J., Coulter, C., Hoffmaster, A.R. and De, B.K. (2010) Identification of an unusual *Brucella* strain (BO2) from a lung biopsy in a 52 year-old patient with chronic destructive pneumonia. BMC Microbiol. 10, 23.
[12] Scholz, H.C., Nockler, K., Gollner, C., Bahn, P., Vergnaud, G., Tomaso, H., Al Dahouk, S., Kampfer, P., Cloeckaert, A., Maquart, M., Zygmunt, M.S., Whatmore, A.M., Pfeffer, M., Huber, B., Busse, H.J. and De, B.K. (2010) *Brucella inopinata* sp. nov., isolated from a breast implant infection. Int. J. Syst. Evol. Microbiol. 60, 801–808.
[13] Occhialini, A., Jimenez de Bagues, M.P., Saadeh, B., Bastianelli, D., Hanna, N., De Biase, D. and Kohler, S. (2012) The glutamic acid decarboxylase system of the new species *Brucella microti* contributes to its acid resistance and to oral infection of mice. J. Infect. Dis. 206, 1424–1432.
[14] Damiano, M.A., Bastianelli, D., Al Dahouk, S., Kohler, S., Cloeckaert, A., De Biase, D. and Occhialini, A. (2015) Glutamate decarboxylase-dependent acid resistance in *Brucella* spp.: distribution and contribution to fitness under extremely acidic conditions. Appl. Environ. Microbiol. 81, 578–586.
[15] Audic, S., Lescot, M., Claverie, J.M. and Scholz, H.C. (2009) *Brucella microti*: the genome sequence of an emerging pathogen. BMC Genomics 10, 352.
[16] Franco, M.P., Mulder, M., Gilman, R.H. and Smits, H.L. (2007) Human brucellosis. Lancet Infect. Dis. 7, 775–786.
[17] Pennacchietti, E., Lammens, T.M., Capitani, G., Franssen, M.C., John, R.A., Bossa, F. and De Biase, D. (2009) Mutation of His465 alters the pH-dependent spectroscopic properties of *Escherichia coli* glutamate decarboxylase and broadens the range of its activity toward more alkaline pH. J. Biol. Chem. 284, 31587–31596.
[18] Capitani, G., De Biase, D., Aurizi, C., Gut, H., Bossa, F. and Grutter, M.G. (2003) Crystal structure and functional analysis of *Escherichia coli* glutamate decarboxylase. EMBO J. 22, 4027–4037.
[19] Rice, E.W., Johnson, C.H., Dunnigan, M.E. and Reasoner, D.J. (1993) Rapid glutamate decarboxylase assay for detection of *Escherichia coli*. Appl. Environ. Microb. 59, 4347–4349.
[20] De Biase, D., Tramonti, A., John, R.A. and Bossa, F. (1996) Isolation, overexpression, and biochemical characterization of the two isoforms of glutamic acid decarboxylase from *Escherichia coli*. Protein Expr. Purif. 8, 430–438.
[21] De Biase, D., Tramonti, A., Bossa, F. and Visca, P. (1999) The response to stationary-phase stress conditions in *Escherichia coli*: role and regulation of the glutamic acid decarboxylase system. Mol. Microbiol. 32, 1198–1211.
[22] Laemmli, U.K. (1970) Cleavage of structural proteins during the assembly of the head of bacteriophage T4. Nature 227, 680–685.
[23] Peterson, E.A. and Sober, H.A. (1954) Preparation of crystaline phosphorilated derivatives of vitamin B6. J. Am. Chem. Soc. 76, 169–175.
[24] Gillespie, J.J., Wattam, A.R., Cammer, S.A., Gabbard, J.L., Shukla, M.P., Dalay, O., Driscoll, T., Hix, D., Mane, S.P., Mao, C., Nordberg, E.K., Scott, M., Schulman, J.R., Snyder, E.E., Sullivan, D.E., Wang, C., Warren, A., Williams, K.P., Xue, T., Yoo, H.S., Zhang, C., Zhang, Y., Will, R., Kenyon, R.W. and Sobral, B.W. (2011) PATRIC: the comprehensive bacterial bioinformatics resource with a focus on human pathogenic species. Infect. Immun. 79, 4286–4298.
[25] Zhao, B. and Houry, W.A. (2010) Acid stress response in enteropathogenic gammaproteobacteria: an aptitude for survival. Biochem. Cell Biol. 88, 301–314.

[26] O'Leary, M.H. and Brummund Jr., W. (1974) PH jump studies of glutamate decarboxylase. Evidence for a pH-dependent conformation change. J. Biol. Chem. 249, 3737–3745.
[27] Cotter, P.D., Gahan, C.G. and Hill, C. (2001) A glutamate decarboxylase system protects *Listeria monocytogenes* in gastric fluid. Mol. Microbiol. 40, 465–475.
[28] Castanie-Cornet, M.P., Penfound, T.A., Smith, D., Elliott, J.F. and Foster, J.W. (1999) Control of acid resistance in *Escherichia coli*. J. Bacteriol. 181, 3525–3535.
[29] Small, P.L. and Waterman, S.R. (1998) Acid stress, anaerobiosis and *gadCB*: lessons from *Lactococcus lactis* and *Escherichia coli*. Trends Microbiol. 6, 214–216.
[30] Sanders, J.W., Leenhouts, K., Burghoorn, J., Brands, J.R., Venema, G. and Kok, J. (1998) A chloride-inducible acid resistance mechanism in *Lactococcus lactis* and its regulation. Mol. Microbiol. 27, 299–310.
[31] Hersh, B.M., Farooq, F.T., Barstad, D.N., Blankenhorn, D.L. and Slonczewski, J.L. (1996) A glutamate-dependent acid resistance gene in *Escherichia coli*. J. Bacteriol. 178, 3978–3981.
[32] Foster, J.W. (2004) Escherichia coli acid resistance: tales of an amateur acidophile. Nat. Rev. Microbiol. 2, 898–907.
[33] Dutyshev, D.I., Darii, E.L., Fomenkova, N.P., Pechik, I.V., Polyakov, K.M., Nikonov, S.V., Andreeva, N.S. and Sukhareva, B.S. (2005) Structure of *Escherichia coli* glutamate decarboxylase (GADalpha) in complex with glutarate at 2.05 angstroms resolution. Acta Crystallogr. D Biol. Crystallogr. 61, 230–235.
[34] Jimenez de Bagues, M.P., Ouahrani-Bettache, S., Quintana, J.F., Mitjana, O., Hanna, N., Bessoles, S., Sanchez, F., Scholz, H.C., Lafont, V., Kohler, S. and Occhialini, A. (2010) The new species *Brucella microti* replicates in macrophages and causes death in murine models of infection. J. Infect. Dis. 202, 3–10.
[35] Jimenez de Bagues, M.P., Iturralde, M., Arias, M.A., Pardo, J., Cloeckaert, A. and Zygmunt, M.S. (2014) The new strains *Brucella inopinata* BO1 and *Brucella* species 83–210 behave biologically like classic infectious *Brucella* species and cause death in murine models of infection. J. Infect. Dis. 210, 467–472.
[36] Hanna, N., Jimenez de Bagues, M.P., Ouahrani-Bettache, S., El Yakhlifi, Z., Kohler, S. and Occhialini, A. (2011) The *virB* operon is essential for lethality of *Brucella microti* in the Balb/c murine model of infection. J. Infect. Dis. 203, 1129–1135.
[37] Gorvel, J.P., Moreno, E. and Moriyon, I. (2009) Is Brucella an enteric pathogen? Nat. Rev. Microbiol. 7 (Author reply 250).
[38] Wattam, A.R., Foster, J.T., Mane, S.P., Beckstrom-Sternberg, S.M., Beckstrom-Sternberg, J.M., Dickerman, A.W., Keim, P., Pearson, T., Shukla, M., Ward, D.V., Williams, K.P., Sobral, B.W., Tsolis, R.M., Whatmore, A.M. and O'Callaghan, D. (2014) Comparative phylogenomics and evolution of the Brucellae reveal a path to virulence. J. Bacteriol. 196, 920–930.
[39] Audic, S., Lescot, M., Claverie, J.M., Cloeckaert, A. and Zygmunt, M.S. (2011) The genome sequence of *Brucella pinnipedialis* B2/94 sheds light on the evolutionary history of the genus *Brucella*. BMC Evol. Biol. 11, 200.
[40] Cozzani, I., Barsacchi, R., Dibenedetto, G., Saracchi, L. and Falcone, G. (1975) Regulation of breakdown and synthesis of L-glutamate decarboxylase in *Clostridium perfringens*. J. Bacteriol. 123, 1115–1123.
[41] Cozzani, I., Santoni, C., Jori, G., Gennari, G. and Tamburro, A.M. (1974) Pyridoxal phosphate-sensitized photoinactivation of glutamate decarboxylase from *Clostridium perfringens*. Biochem. J. 141, 463–468.
[42] Cozzani, I. and Bagnoli, G. (1973) The subunits of L-glutamate decarboxylase from *Clostridium perfringens*. Ital. J. Biochem. 22, 36–45.
[43] Cozzani, I. and Bagnoli, G. (1971) Reversible resolution of glutamate decarboxylase from *Clostridium perfringens*. Ital. J. Biochem. 20, 179–190.
[44] Cozzani, I., Misuri, A. and Santoni, C. (1970) Purification and general properties of glutamate decarboxylase from *Clostridium perfringens*. Biochem. J. 118, 135–141.
[45] Tennant, S.M., Hartland, E.L., Phumoonna, T., Lyras, D., Rood, J.I., Robins-Browne, R.M. and van Driel, I.R. (2008) Influence of gastric acid on susceptibility to infection with ingested bacterial pathogens. Infect. Immun. 76, 639–645.